

Application of the Global Positioning System to the Measurement of Overhead Power Transmission Conductor Sag

C. Mensah-Bonsu
Student Member

U. Fernández
Student Member

G. T. Heydt
Fellow

Y. Hoverson
Non-Member

J. Schilleci
Senior Member

B. Agrawal
Fellow

Center for the Advanced Control of Energy and Power Systems
Arizona State University, Tempe, AZ

Entergy
New Orleans, LA

Arizona Public Service
Phoenix, AZ

Abstract This paper describes a method to directly measure the physical sag of overhead electric power transmission conductors. The method used relies on the Global Positioning System (GPS) used in the differential mode. The *direct measurement* of sag is a main advantage of the concept. The digital signal processing required is described in detail in a four level configuration. Typical accuracy, response time, problems, strengths and weaknesses of the method are also described.

Keywords: *Global Positioning System; overhead conductors; sag; dynamic line rating; transmission engineering; Open Access Same Time Information System(OASIS).*

1. Overhead conductor ratings

Under deregulation of the power industry in the United States, electric utilities are under pressure to make optimum use of their existing facilities of which the overhead transmission system is usually a principal component. Overhead conductors form the backbone of power transmission systems. The ratings of circuits are critical to system capability. Real time conductor rating holds promise for the maximization of system transfer capability.

The transmission capacity of overhead conductors depends on the ambient temperature, wind speed, wind direction, incident solar radiation, limiting physical conductor characteristics, and conductor configuration / geometry. The conductor load capacity is computed *statically* or *dynamically*. In the static case, a worst case weather condition is assumed while in the dynamic case the actual weather condition is taken into account. In either case, the conductor load must produce a conductor temperature so that there is no loss of strength by annealing or creep. One must operate the circuit so that the mandated clearances are not violated. Experience in some utilities shows that the clearance of an overhead conductor is a key factor limiting its thermal capacity especially in regions of high intercon-

nection. An ultimate measure of the conductor rating is the physical sag of the conductor and the continuous monitoring of the conductor clearance may improve system operation. This paper considers the use of a GPS based measurement system for overhead conductor sag – based on tests using a laboratory breadboarded prototype.

Traditionally, conductor sag has been considered by indirect measurements. Recently commercialized techniques include the physical measurement of conductor surface temperature using an instrument mounted directly on the line, and a second instrument that measures conductor tension at the insulator supports. These measured parameters can be used to estimate conductor sag. The pertinence of conductor sag to circuit operation relates to the calculation of a *dynamic thermal rating* of the line, considering the ambient conditions and present operating regime [1-5]. In a deregulated electric utility environment, transmission circuit ratings assume renewed importance because some companies are marketing transmission access. A widely used system for transmission capacity sales is known as OASIS. To be able to rapidly and accurately determine the dynamic transmission rating of a circuit has obvious pecuniary value in OASIS.

2. The Global Positioning System

Based on a constellation of 24 satellites, the Navigation Satellite Timing and Ranging (NAVSTAR) GPS was developed, launched and maintained by the United States government as a worldwide navigation and positioning resource for both military (i.e. precise positioning service) and civilian (i.e. standard positioning service) applications. The method relies on accurate time-pulsed radio signals in the order of nanoseconds from high altitude Earth orbiting satellites of about 11,000 nautical miles, with the satellites acting as precise reference points. These signals are transmitted on two carrier frequencies known as the L1 and L2 frequencies. The L1 carrier is 1.5754 GHz and carries a pseudorandom code (PRC) and the status message of the satellites. There exist two pseudorandom codes; the coarse acquisition (C/A) and the precise (P) codes. The L2 carrier is 1.2276 GHz and is used for the more precise military PRC. The signals from four or more satellites are received by a specially designed GPS receiver, and the following simultaneous equations are solved,

$$(X_{sk} - X_{rj})^2 + (Y_{sk} - Y_{rj})^2 + (Z_{sk} - Z_{rj})^2 = (R_k - dT)^2$$
$$k = 1, 2, \dots, n \quad n \geq 4 \quad (1)$$

where (X_{sk}, Y_{sk}, Z_{sk}) represents the k th satellite position, (X_{rj}, Y_{rj}, Z_{rj}) denotes the unknown j th receiver position, R_k denotes the range to the k th satellite and dT is the unknown

receiver clock bias converted to distance. This gives the longitude and latitude of the receiver (i.e., effectively x and y), the altitude of the receiver (effectively z), and the time that the measurement was made, t . Interestingly, the GPS transmission is made at low power level (the signal strength at the point of reception is about -90 to -120 dBm); at this power level, the signal to noise ratio is very low at the surface of the Earth. The attenuation of the noise is accomplished by averaging the received signal: the noise is averaged and a distinctively coded signal appears as an output. The averaging process as well as the solution of Equation (1) is the main time limiting process that determine how often a GPS measurement can be made.

Perhaps the most often asked question about GPS technology relates to its accuracy. The ultimate accuracy of position measurements made using the GPS depend on a variety of factors (e.g., the type of measurement made, x , y , or z ; ionospheric and tropospheric conditions; government inserted error effected as a security measure; number of satellites in view; receiver equipment used; digital signal processing of the received signal; surface features; reflection of signals; and other factors). Table (1) summarizes some of these interacting factors and the approximate error. In Table (1), a differential mode of measurement is also shown, and this is discussed later. The greatest source of error is the intentional insertion of error through a subsystem known as Selective Availability (SA): this error is inserted by the government as a security measure. Authorized non-civilian users of a special high accuracy mode of operation have a special mechanism to decode the SA and eliminate the intentional error.

Table (1) Approximate GPS position measurement error (total) contributing factors and estimates

Error contributing factor	Approximate error (m)	
	Standard GPS	DGPS
Selective availability (SA)	30.0	0.0
Ionospheric variation	5.0	0.4
Inaccurate orbital path	2.5	0.0
Satellite clock	1.5	0
Multipath signal error	0.6	0.6
Tropospheric variation	0.5	0.2
Receiver noise	0.3	0.3

The differential GPS (DGPS) mode is generally used in order to decrease the SA error. This mode consists of the use of two GPS receivers, the *base* and the *rover*. The actual position of the base is known (e.g., by precise surveying) and compared to the readings received at the same base point. With the estimated error, the readings obtained at the rover can be compensated by simple subtraction. The value of the DGPS technique is a marked increase in instrument accuracy with little degradation of time requirement. The main drawback of the DGPS technique is the requirement of a second GPS receiver and corresponding communication equipment between the base and rover instruments. Also, if the rover and base instruments are

widely separated, the solution accuracy will degrade. The term *direct* DGPS is used to refer to a GPS configuration in which the position and time measurements are available at the rover station. The term *inverse* DGPS refers to a DGPS instrument in which the results are available at the base station. Table (2) shows typical position accuracy of GPS and DGPS [7 – 9].

Table (2) Typical position accuracy of GPS in (m)

	Standard GPS	Differential GPS
Horizontal	50	1.3
Vertical	78	2.0
Three dimensional	93	2.8

3. GPS Measurement of overhead conductor sag

Figure (1) shows a proposed basic configuration of a DGPS method to measure overhead transmission conductor position and hence, sag. Inverse DGPS technology is used. Normally only one phase of a circuit would be instrumented in a critical span. From the base station, hard-wire is used to bring position data to power system operators. Alternately, the base station may be at the operations center itself. There is a considerable data processing burden in the implementation of the DGPS: this is needed to attenuate noise and enhance accuracy. This burden is calculable in real time using serial on-line processing. The main time resolution limitations of the instrument are the calculation of the (x, y, z, t) from the GPS signal and bad data rejection described in the next section.

4. Data processing from the GPS

The accuracy of GPS measurements depends heavily on the configuration of the receiver(s) (e.g., standard GPS or differential), parameters that influence error in measurements, the number and position of the satellites in view, and the digital signal processing of the GPS measurements. The fundamental required data processing is the solution of the time-distance linear equations,

$$distance = (velocity) (time),$$

for the four or more GPS measurements. The form of these equations is shown in Equation (1). These equations are usually solved recursively using a previously solved case as an initialization. This is shown in Figure (2) as the

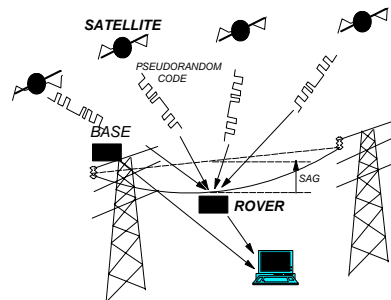


Fig. (1) Basic DGPS configuration for conductor sag measurement

first level of required digital processing. In the case of the application of DGPS measurements, the application of the correction signal from a base station receiver is also fun-

damental. This is shown in Figure (2) as a second level signal processing. The first and second levels of processing are done entirely by the GPS engine. The central focus of interest in the measurement of overhead transmission conductor sag is in the measurement of altitude, that is $z(t)$.

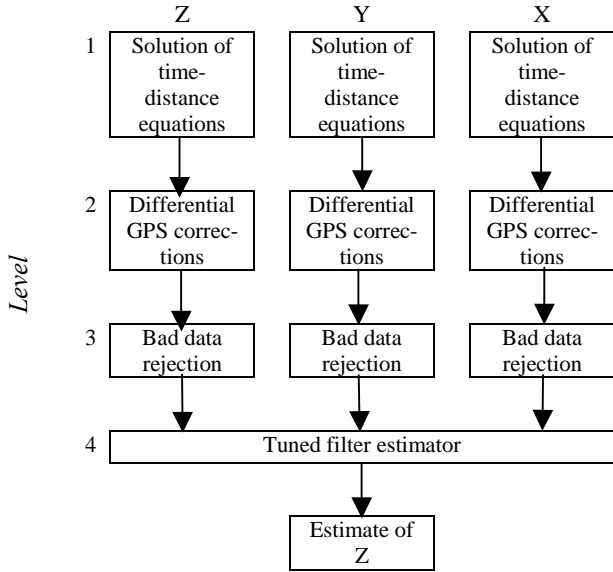


Fig. (2) Depiction of four levels of digital signal processing required for GPS measurements

In level 3 of the data processing, bad data rejection is used. Bad data result from a variety of causes – some not fully understood. The momentary loss of some satellites from view will negatively impact the measurement accuracy. Also, momentary interference and signal reflections may degrade accuracy. In addition, the ambient noise impacts solution accuracy. Other error mechanisms may also create single datum values that are erroneous.

Identification of bad data is accomplished through the use of the identification of a measurement which differs from the mean value (of x , y , or z as appropriate) by greater than preset tolerance values $k\sigma_x$, $k\sigma_y$, $k\sigma_z$ respectively where the σ values denote the sample standard deviation values of x , y , and z as measured in a moving window of width T . The bad datum is replaced with the window mean. Parameter k is chosen to obtain the proper rejection rate, and the window width T is chosen shorter than the expected duration of residence of the conductor in a given position. Typical values for the present application are $k = \pm 1.0$ and $T = 30$ s. Considerations in the selection of these parameters are: expected wind conditions and movement of the conductor, operators' requirements of real time values; and accuracy of the readings. It should be pointed out that choosing a large T implies the introduction of certain delay, since the readings of the previous positions may be still in the window. On the other hand, a very short window width will produce no rejection.

The effect of the bad data rejection can be observed in Figure (3), which shows the cumulative distribution of the absolute value of the error computed from measurements

taken for a set of known positions. The results depicted in Figure (3) were obtained experimentally using a 12 channel DGPS receiver at a surveyed position near Phoenix, AZ at about 359 m above mean sea level taking readings at the rate of one per second.

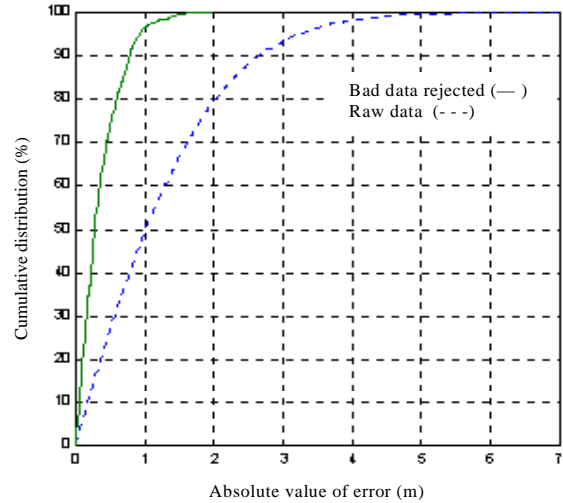


Fig. (3) Effect of bad data rejection

A fourth level of digital signal processing is depicted in Figure (2). Note that the measurements are made at approximately 0.9 s intervals, and the measured data is available at discrete values of time. For this reason, it is convenient to refer to the measured set of data as $x(k)$, $y(k)$, $z(k)$. The time measurement is not used in this application. Field trials of a prototype instrument indicate that errors in x and y often occur simultaneously with errors in z . This suggests that measured x and y could provide additional information for corrections in z . In this fourth level of signal processing, two different techniques have been tested: a least squares estimator (LSE) and an artificial neural network estimator (ANNE). Both are separately used as tuned filter estimators that are trained (tuned) using a known data set. Surveyed data are used to provide a set of $[x_k, y_k, z_k]$ data which are used to select parameters of the estimators such that the error in the known set is minimized. For testing purposes, the data set allows the comparison of estimated x , y , z to known values thereby providing an estimate of the instrument accuracy.

In trying to capture the nonlinear behavior of the error, the LSE adopted is formulated as,

$$\hat{z}(n) = Ax(n) + By(n) + Cz(n) + Dx^2(n) + Ey^2(n) + Fz^2(n)$$

where $x(n)$, $y(n)$, $z(n)$ are the sampled readings at certain time that produce the corresponding vertical measurement estimation $\hat{z}(n)$. Using the set of measurements $x(n)$, $y(n)$, $z(n)$ taken for a set of known altitude z_o and replacing $\hat{z}(n)$ with z_o the above equation can be expressed in matrix form as,

$$Z_{Known} = X\Theta$$

where $\Theta = [A B C D E F]^T$. The parameters $[A, B, C, D, E, F]$ are computed using simple state estimation (i.e.,

least squares parameter estimation). One formulation involves the Moore-Penrose pseudoinverse of the matrix X [10].

The ANNE is implemented using a time lag feed forward network [11]. In this configuration, contrary to the LSE, p previous readings of x , y and z are used to estimate z . A two-weighted layer network is used, consisting of h neurons in the hidden layer and one output layer. A sigmoid function, specifically the logistic function [11] is employed as the activation function of the hidden neurons, while the output neuron employs a linear function. The optimum values of p and h are determined in the tuning process. A schematic of the network is shown in Figure (4).

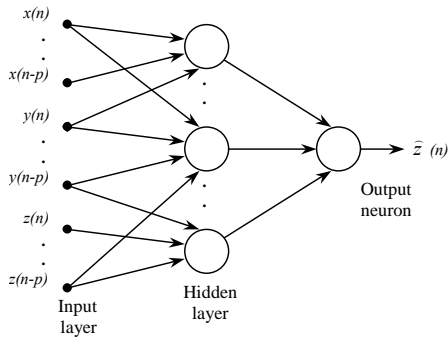


Fig. (4) ANN parameter estimator to correct $z(n)$ data from a DGPS measurement

Some results of field testing and the details of the signal processing techniques described here are shown in the Appendix. Note that through the use of a least squares estimator, accuracy within 21.5 cm was obtained 70% of the time, and using an artificial neural network estimator, an accuracy of at least 19.6 cm is obtained for 70% of the time (see Table (A1)).

5. Power supply and communications link

For a practical sag measurement instrument, in addition to the digital signal processing outlined above, there is the matter of instrument power supply and the communication link between the base and rover units. Based on a popular commercial GPS receiver, the power supply requirements for the base and rover instruments are shown in Table (3). The power requirements at the base station are derived from conventional sources. At the rover, power must be derived from the overhead conductor itself. This concept has been commercialized in many applications, and laboratory tests revealed that the technology is easily implemented. Figure (5) shows one configuration based on a current transformer (CT) design. Experience shows that voltage regulation of the GPS receiver supplies is essential. Communication between the rover and base station is accomplished using standard digital communications technologies. A typical communication link consists of ‘on-off’ amplitude modulation for the communication channel, implemented in the Industrial Scientific and Medical (ISM) band, 902 - 928 MHz. The design tested in the laboratory is effectively a serial port connection via radio. Figure (6)

shows a possible configuration. The frequency source in this design is derived from a voltage controlled oscillator (VCO) which is held at the proper frequency by a phase locked loop circuit. The ultimate frequency source is a quartz crystal (XTAL).

Table (3) Instrument power requirements (typical)

Unit	Component	Typical power requirements (DC)		
		V (volts)	I (amps)	P (watts)
Rover	GPS receiver	12	2	24
	Digital (serial) data transmitter	12	2	24
	Digital (serial) data receiver	12	0.2	2.4
Base	GPS receiver	12	2	24
	Digital (serial) data transmitter	12	5	60
	Digital (serial) data receiver	12	0.2	2.4

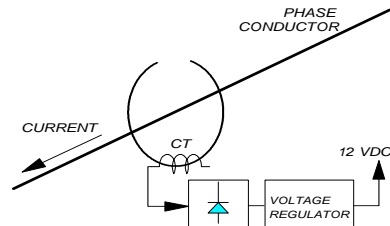
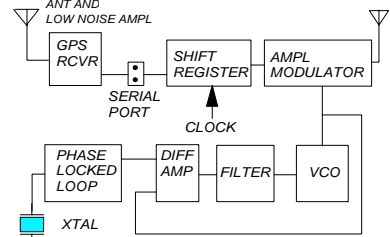
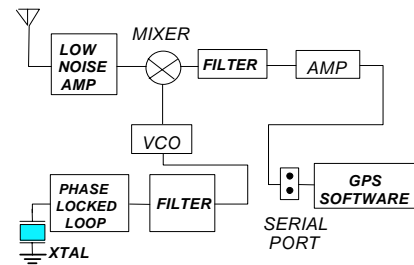


Fig. (5) Power supply for the rover unit: a magnetic ring is clamped around the conductor to be instrumented.



(a) GPS receiver / rover transmitter



(b) Base station receiver

Fig. (6) Communication between the rover and base stations

An important issue in the present application is the performance of the communication link in a high voltage environment (and, perhaps more serious, the 1.5 GHz band reception of the GPS signal at the rover). Experiments

have been done to determine the difficulties in these areas and the main conclusion is that corona creates potentially intolerable conditions for radio reception in the 930 MHz and 1.5 GHz bands. There may also be some degree of ‘saturation’ in the receiver front end first stages, but the use of low noise amplifiers, standard in ISM and GPS technologies, seems to be adequate. It is important that the radio receivers at the rover be far from any corona. The receiver should be ‘shielded’ by instrument packaging that is smooth and corona free.

6. Dynamic thermal line ratings

As previously discussed, sag information is valuable in order to determine dynamic thermal rating of overhead conductors. In present dynamic thermal rating methods, the sag information is an *output*, but in this new approach, the sag information is an *input*, consequently the rating computation method must be reviewed. Although it is beyond the scope of this paper, a tentative method is outlined: Figure (7) summarizes a procedure to utilize sag information and translate it to conductor rating.

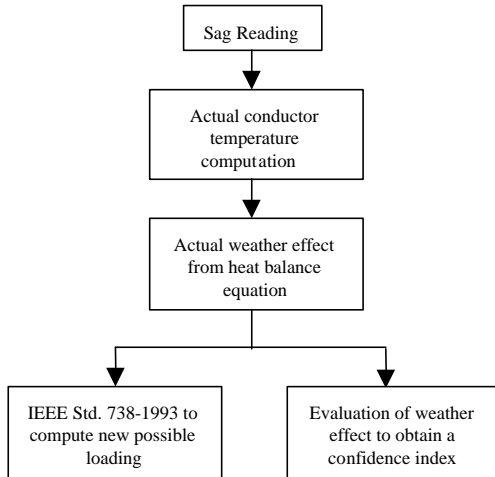


Fig. (7) Computation of dynamic thermal rating based on sag information

For specified values of conductor physical characteristics, i.e., weight per unit of length, modulus of elasticity and linear coefficient of expansion, and for given installation conditions of the conductor, the new conductor temperature can be computed [12]. With the knowledge of the conductor temperature and current, the net weather influence in the heat balance equation [2] can be evaluated,

$$q_s - q_c - q_r = mC_p \frac{dT_c}{dt} + I^2 R(T_c) \quad (3)$$

where q_s , q_c , q_r , mC_p , I , R , and T_c represent the solar heat gain, convection heat loss, radiated heat loss, total heat capacity, conductor current, conductor resistance, and the conductor temperature respectively. The variations in the terms of the left side of Equation (3) could be computed for known variation of the conductor temperature using the equations and tables suggested in [2]. Using the estimated initial net weather effect, and with the ability to compute changes in it, Equation (3) could be again solved for a step

increase in current. Computation in this way, the maximum current increase that corresponds to the maximum allowable temperature is found. It should be pointed out that the variation in the net weather effect is assumed to be caused only by an increase in the conductor temperature and not in weather conditions.

Using continuous monitoring of the current and the conductor temperature (via sag information), the net weather effect ($q_s - q_c - q_r$) can be computed. A highly variable weather condition implies that the maximum current computed may not be reliable. On the other hand, if the net weather is static, confidence is higher. For this reason a confidence index, based on the variance of the net weather effect for different time windows is suggested.

Real time measurements of conductor sag have the potential of being accurately converted to real time, dynamic line ratings; these dynamic ratings are then useable in connection with systems studies to determine the maximum transmission capacity of circuits. The OASIS system is, in effect, a market for this transmission capacity, and it is possible that accurate, on-line, dynamic line ratings may have considerable value.

7. Conclusions

The main conclusion of this study is that DGPS technology is feasible for the direct instrumentation of overhead power line conductor sag measurement. The accuracy of such an instrument is in the range of 19.6 cm 70% of the time. The method utilizes two GPS receivers, one as a base station which must be at an accurately surveyed location. The instrument can be designed such that the rover receiver operating power is taken from the line. Care must be taken in the design of the instrument package because of the potential of interference from corona. The main digital signal processing needed to obtain accurate z measurements are bad data rejection, least squares parameter estimation, or artificial neural network filtering.

Although the subject of dynamic line ratings is not considered in this paper, it is believed that real time sag measurement can be translated into real time, dynamic circuit ratings, and this is expected to have value in the sale of transmission capacity.

Acknowledgements

The authors acknowledge the assistance of colleagues at Entergy and the Arizona Public Service Company. Professors E. Burns, R. Farmer and G. Karady of ASU and D. Selin of APS are gratefully acknowledged. Alex Hunt of ASU designed the DGPS receiver circuit, and several students assisted in the power supply and communications link designs. John Wells of the United States Navy is acknowledged for power supply design. The generous help of R. Faulkner and A. Carbognin and the loan of GPS receivers from NovAtel Inc., Calgary, were critical to the work reported. The work was done under the auspices of the Center for the Advanced Control of Energy and Power Systems.

References

- [1] G. Ramon, IEEE Task Force Chairman: "Dynamic thermal line rating summary and status of the state-of-the-art technology," IEEE Transactions on Power Delivery, v. PWRD-2, No. 3, July 1987, pp. 851-856.
- [2] IEEE Std. 738-1993, IEEE Standard for Calculating the Current-Temperature Relationship of Bare Overhead Conductors, New York, 1993.
- [3] T. Seppa, "Accurate ampacity determination: temperature-sag model for operational real time ratings," IEEE Transactions on Power Delivery, v. 10, No. 3, July 1995, pp. 1460-1466
- [4] U. Fernández, C. Mensah-Bonsu, J. Wells, G. Heydt, "Calculation of the maximum steady state transmission capacity of a system," Proceedings of the 30th North American Power Symposium, Cleveland, Ohio, October 19-20, 1998, pp. 300-305.
- [5] D. Douglas, A. Edris, "Real-time monitoring and dynamic thermal rating of power transmission circuits," Transactions on Power Delivery, v. 11, No. 3, July 1996, pp. 1407-1415
- [6] B. J. Cory, P. F. Gale, "Satellites for power system applications," IEE Power Engineering Journal, v. 7 No. 5, October 1993.
- [7] J. Hurn, *Differential GPS Explained*, Trimble Navigation Ltd., Sunnyvale, CA 1993.
- [8] E. Kaplan, *Understanding GPS: Principles and Applications*, 1996.
- [9] T. Gray, *NAVSTAR GPS and DGPS*, CSI Inc., 1997.
- [10] G. Heydt, *Computer Analysis Methods for Power Systems*, Stars in a Circle Publications, Scottsdale, AZ, 1998.
- [11] S. Haykin, *Neural Networks: A Comprehensive Foundation*, 2nd Edition, Prentice Hall, New York, NY, 1999.
- [12] D. G. Fink, H. W. Beaty (Editors), *Standard Handbook for Electrical Engineers*, 13th Edition, McGraw-Hill, 1993.

Appendix

Signal processing results

In order to test the above described signal processing procedures, a series of tests were done. One exemplar test is described as taking DGPS readings for ten known elevations (stations), collocated in longitude and latitude. The altitude difference between stations varies between 0.10 to 1.0 m. An average of 1800 readings were taken for each station. From the ten stations, five were used to tune the estimators and the rest were used to test the performance of the estimators in the presence of data not previously seen. The bad data rejection in the third level has been computed using values of $k = 1$ and $T = 30$ s. These have presented a good performance regarding excessive number of data rejection and the response time, as explained previously. For the ANNE, several configurations have been explored regarding the number of neurons in the hidden layer. Good results were obtained for $h = 4$. In all cases, the number of previous readings used have been $p = 9$. With the configurations described the results obtained are summarized in Figure (A1).

It can be seen that for a 90% confidence the LSE and ANNE present respectively an accuracy of 41.9 cm and 37.4 cm. For 70% confidence, the respective accuracy are 21.5 cm and 19.6 cm. Table (A1) summarizes the accuracy obtained with the respective confidence index. In Table (A1), note that there is an additional 5 cm uncertainty in the antenna position, and at least 5 cm potential survey error. It is expected that the inaccuracies tabulated are conservative. It can be seen that the ANNE presents

slightly better results. However, both estimator present similar performance.

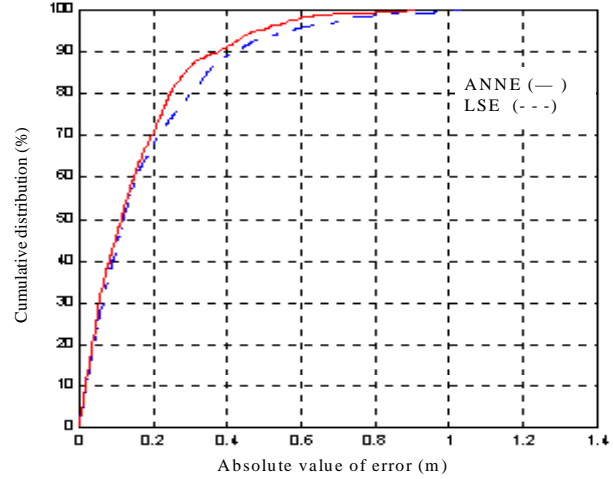


Fig. (A1) Cumulative error for LSE and ANNE

Table (A1) Accuracy achieved by LSE and ANNE

Confidence Index (%)	Absolute error (cm)			
	Raw data	Bad data rejected	LSE	ANNE
90	264.4	78.5	41.9	37.4
80	201.8	58.9	30.1	24.5
70	161.1	45.5	21.5	19.6
60	128.9	34.9	15.4	14.6
50	100.6	27.9	11.8	11.4

Biographies

Chris Mensah-Bonsu was born in Kumasi, Ghana. He received Masters degrees in Control Systems and Electric Power Engineering from Cleveland State University and the Higher Institute of Mechanical and Electrical Engineering, Varna, Bulgaria, respectively. He is currently a graduate research associate at Arizona State University completing requirements for the Ph.D. degree.

Ubaldo Fernández Krekeler is from Asunción, Paraguay. He obtained the degree in Ingeniería Electromecánica from the Universidad Nacional de Asunción. He is a winner of a Fulbright Fellowship award. He is presently a graduate research assistant at Arizona State University where he expects to receive the MSEE degree in 1999.

Gerald Thomas Heydt holds the Ph.D. from Purdue University. He is a Fellow of the IEEE, a member of the National Academy of Engineering, and recipient of the 1995 Power Engineering Society "Power Engineering Educator of the Year" award. Dr. Heydt is presently a Professor of Electrical Engineering and Center Director at ASU.

Yuri Hoverson is from Scottsdale, Arizona. He has experience with the U. S. Navy. Mr. Hoverson is completing the requirements of the BSME degree at Arizona State University. He is the 1999 recipient of the Salt River Project Energy and Environment Scholarship.

John Schilleci is a native of New Orleans. He holds a BSEE degree from Louisiana State University and is a Senior Member of IEEE. He has been in the electric utility business for the last 32 years with experience in Substation, Transmission, Distribution, Metering and Communications. He is an adjunct faculty member of the Electrical Engineering Department at the University of New Orleans.

Baj L. Agrawal was born in Kalaiya, Nepal. He received his BS in Electrical Engineering from Birla Institute of Technology and Science, India and his Masters and PhD in Control Systems from the University of Arizona. Dr. Agrawal joined Arizona Public Service Company in 1974 where he is currently working as a Senior Consulting Engineer. He is registered professional engineer in the state of Arizona and is a member of the IEEE SSR Working Group.